Proceedings of ASME Turbo Expo 2011
GT2011
June 6-10, 2011, Vancouver, British Columbia, Canada

GT2011-45033

ANALYTICAL INVESTIGATION OF THE EFFECTS OF INDUCTION MOTOR TRANSIENTS ON COMPRESSOR DRIVE SHAFTS

Anand Srinivasan
Cameron Process and
Compression Systems
Buffalo, NY, USA

ABSTRACT

Centrifugal compressors driven by induction motors are most common in the turbomachinery industry. When sudden transients occur in the driver due to upsets in electrical supply to the motor, the air-gap torque generated by the motor undergoes a transient spike. This in turn gets transmitted through the coupling to the drive-shaft of the driven equipment, causing momentary high spikes in vibration that are torsional in nature, and can sometimes result in shaft torques that can create catastrophic damage to driven equipment components. In order to analytically predict these peak torques that can occur during transients, a complete drive-train torsional model needs to be created for the mechanical system, and the driving torque values need to be derived from the motor electrical system of equations. Various line faults are possible with induction motor driven equipment. A generalized analytical procedure based on motor electrical parameters to predict the peak shaft torques of compressor drive shafts is investigated in this paper. The effects of shaft transients due to 3-phase short circuits and reclosures are analyzed. The simulation has been performed for an industrial compressor train, and has been presented from a mechanical system point of view, rather than electrical. Comparisons and inferences are also made based on the simulation results.

INTRODUCTION

A typical turbomachinery drive train assembly consists of a 3-phase induction motor driver that is connected to a compressor by a coupling. The simplified model of an induction motor consists of a stator and a rotor winding. The resistances and inductances of the stator and rotor windings govern the electrical output. The voltage applied at the stator induces a flux across the rotor windings by transformer action via the mutual inductance coil, thus creating an electromagnetic effect in the gap between the stator and the rotor. The torque generated by this induced voltage in the gap is known as the air-gap or electromagnetic torque of the motor. When a load (such as a compressor) is connected to this motor, the air-gap torque generated by the motor drives the compressor. At steady state, the electromechanical torque output by the motor is equal to the shaft torque demanded by the compressor. However, transient upsets can occur in the motor due to various factors, some of the most common being short circuits in the rotor windings, dips or surge in line-voltage supply, and reconnection of the motor to power supply after a power failure. Such transients in the motor torque can create a sudden change in the air-gap torque, which can get transmitted to the shaft of the driven equipment as torsional excitations. The frequency of these torsional oscillations is governed by the torsional natural frequency of the drive train. The length of time taken for these oscillations to die down depends on the damping provided by the coupling and the inherent damping of steel.

Daugherty [1, 2], Mruk & Halloran [3] and Shaltout & Al-Omoush [4] have researched the topic of induction motor transients related to reclosures in the past. Hizume [5] has researched the topic of high speed reclosures on a turbine-generator system. Hizume's paper provides an excellent review of the basics of reclosure that is aimed towards mechanical engineers. More recently, Melfi & Umans [6] discussed the transient nature of line starting of induction motors. However, there appears to be minimal research in the mechanical literature that covers both reclosure and 3-phase fault transients, and its comparison of torques with start-up transients.

This paper investigates the analytical model to predict shaft torque magnitudes due to sudden transients arising from the motor. The simulated effects of a 3-phase short circuit and reclosure transients are studied, and inferences are made on the nature of the magnitudes of the shaft torques for each case. The magnitudes of these torque upsets are compared to the transients during start-up of the drive train.

NOMENCLATURE

C_1, C_2 damping (N-s-m, lb-s-ft)
f line frequency (50 or 60 Hz)
FLT_{c1}, FLT_{c2} full load compressor torque (N-m, ft-lb)
I_s, I_r stator and rotor currents (PU)
J_m, J_{c1}, J_{c2} polar moment of inertia of the motor, compressor1 and compressor2 (kg-m-s^2, lb-ft-s^2)
K_1, K_2 coupling torsional stiffness (kg-m/rad, lb-ft/rad)
L_s, L_r, L_{sr} stator, rotor and 3-phase equivalent mutual inductance (PU)
L_{mu} 2-phase mutual inductance (PU)
$octc$ open circuit time constant (s)
$Poles$ number of poles
R_s, R_r stator and rotor resistances (PU)
t time (s)
T_{ag} air-gap torque (PU)
T_{s1}, T_{s2} shaft torques (PU)
V_{sup} supply voltage (PU)
V_m motor flux voltage (PU)
V_s, V_r stator and rotor voltages (PU)
V_{res} resultant voltage due to trapped flux (PU)
X_s, X_r, X_{mu} stator, rotor and mutual reactances (PU)
β phase angle between supply and flux voltage (rad)
θ_r instantaneous angular position – electrical (rad)
θ_m instantaneous angular position – mechanical (rad)
θ_{c1}, θ_{c2} angular position of compressor shafts (rad)
λ_s, λ_r stator and rotor flux (PU)
ω nominal rated speed (rad/s) = $2\pi f$
ω_{c1}, ω_{c2} instantaneous compressor angular speeds (rad/s)
ω_r, ω_m motor electrical and mechanical angular speeds (rad/s)
k integer, superscript denotes phase – 1, 2 or 3

ANALYTICAL MODEL

The equations for a 3-phase induction motor, as adapted from Daugherty [1] and Krause et al [7], can be written as follows. The stator voltages for each of the phases can be represented by Eq. (1), where the superscript k denotes the appropriate phase (1 for phase a, 2 for b and 3 for c).

$$V_s^k = R_s I_s^k + \frac{d}{dt}\lambda_s^k, k = 1,2,3 \tag{1}$$

The stator induces a voltage in the motor rotor via the magnetic flux induced in the air-gap between the stator and the rotor. The equations for the rotor voltages are thus given by

$$V_r^k = 0 = R_r I_r^k + \frac{d}{dt}\lambda_r^k, k = 1,2,3 \tag{2}$$

The rotor voltage is zero since no voltage is directly applied to the rotor windings. The fluxes induced in the stator and rotor are given by Eq. (3) and (4):

$$\lambda_s^k = L_s I_s^k + L_{mu}\sum_{n=1}^{3} I_r^n \cos\left[\theta_r + (n-1)\frac{2\pi}{3}\right] \tag{3}$$

$$\lambda_r^k = L_r I_r^k + L_{mu}\sum_{n=1}^{3} I_s^n \cos\left[\theta_r - (n-1)\frac{2\pi}{3}\right] \tag{4}$$

Differentiating Eq. (3) and (4) with respect to time, substituting in Eq. (1) and (2), and re-writing results in Eq. (5) and (6),

$$\begin{aligned} L_s\frac{d}{dt}I_s^k + L_{mu}\sum_{n=1}^{3}\frac{d}{dt}I_r^n \cos\left[\theta_r + (n-1)\frac{2\pi}{3}\right] \\ = V_s^k - R_s I_s^k \\ + L_{mu}\omega_r\sum_{n=1}^{3} I_r^n \sin\left[\theta_r + (n-1)\frac{2\pi}{3}\right] \end{aligned} \tag{5}$$

$$\begin{aligned} L_r\frac{d}{dt}I_r^k + L_{mu}\sum_{n=1}^{3}\frac{d}{dt}I_s^n \cos\left[\theta_r + (n-1)\frac{2\pi}{3}\right] \\ = -R_r I_r^k \\ + L_{mu}\omega_r\sum_{n=1}^{3} I_s^n \sin\left[\theta_r - (n-1)\frac{2\pi}{3}\right] \end{aligned} \tag{6}$$

where the inductances, as defined in [1], are represented by Eq. (7-9).

$$L_{mu} = \frac{2}{3}\frac{X_{mu}}{\omega} = \frac{2}{3}L_{sr} \tag{7}$$

$$L_s = \frac{X_s}{\omega} + L_{sr} \tag{8}$$

$$L_r = \frac{X_r}{\omega} + L_{sr} \tag{9}$$

Equations (5) and (6) are matrices of the form

$$\begin{aligned} \{L\}_{6x6}\frac{d}{dt}\{I\}_{6x1} = \{V\}_{6x1} - \{R\}_{6x1}\{I\}_{6x6} \\ + \omega_r\{L\}_{6x6}\{I\}_{6x1} \end{aligned} \tag{10}$$

The current derivative in Eq. (10) is a function of both stator and rotor currents, and time. Multiplying both sides by $\{L\}^{-1}$, Eq. (10) can be expressed in the form of Eq. (11) such that it represents the derivatives of current in each of the phases for the stator and rotor.

$$\frac{d}{dt}f(I_s, t) = f(I_s, I_r, t) \tag{11}$$

Equation (11) can be solved for the currents by performing a numerical integration using the 4th order Runge Kutta (RK) solver at each time step. Once $\{I\}_{6x1}$ is determined, the $\{\lambda\}_{6x1}$ matrix can be calculated using Eq. (3) and (4). However, the solution can be obtained only after the coupled set of equations between the motor and the compressor torques are defined. The air-gap torque generated by the motor is given by Eq. (12).

$$T_{ag} = -\frac{\omega}{3\sqrt{3}}[\lambda_r^1(I_r^2 - I_r^3) + \lambda_r^2(I_r^3 - I_r^1) + \lambda_r^3(I_r^1 - I_r^2)] \tag{12}$$

A typical motor-compressor drive train for a dual gearbox integral geared compressor arrangement consists of a motor driving two compressors, connected by a shaft and a coupling (one for each compressor). Refer Fig. 1, represented with the respective angular velocities. The equations of motion for the mechanical counterparts are written in the form of Eq. (13), as described in Vance [8].

$$\begin{Bmatrix} \dot{\theta}_p \\ \dot{\omega}_p \end{Bmatrix} = \{A\} \begin{Bmatrix} \theta_p \\ \omega_p \end{Bmatrix} \tag{13}$$

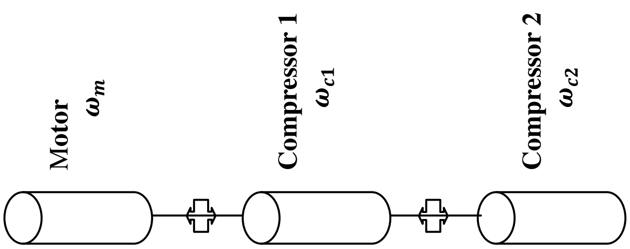

Figure 1: Drive train arrangement

Expressing the mechanical quantities in this form once again facilitates easy use of the RK solver. The detailed mechanical system of equations for the motor-compressor1-compressor2 drive train can be written in the form of Eq. (14-19).

$$\frac{d\theta_m}{dt} = \omega_m \tag{14}$$

$$J_m \frac{d\omega_m}{dt} = T_{ag} - C_1(\omega_m - \omega_{c1}) - K_1(\theta_m - \theta_{c1}) \tag{15}$$

$$\frac{d\theta_{C1}}{dt} = \omega_{c1} \tag{16}$$

$$J_{c1} \frac{d\omega_{c1}}{dt} = -FLT_{c1} - C_1(\omega_{c1} - \omega_m) - C_2(\omega_{c1} - \omega_{c2}) - K_1(\theta_{c1} - \theta_m) - K_2(\theta_{c1} - \theta_{c2}) \tag{17}$$

$$\frac{d\theta_{C2}}{dt} = \omega_{c2} \tag{18}$$

$$J_{c2} \frac{d\omega_{c2}}{dt} = -FLT_{c2} - C_2(\omega_{c2} - \omega_{c1}) - K_2(\theta_{c2} - \theta_{c1}) \tag{19}$$

The electrical rotor position θ_r and the mechanical position θ_m are related to each other by the number of pole pairs and can be represented by Eq. (20).

$$\theta_r = \theta_m \frac{Poles}{2} \tag{20}$$

A similar relationship holds true for ω_r and ω_m. The complete set of non-linear equations for the electrical system and the mechanical system can now be solved to obtain the transient response solution.

The voltage applied to each phase for a 3-phase system is a sinusoidal (or cosine) function [7] with a frequency equal to the line frequency and a peak amplitude of $\sqrt{2}$ times the PU supply voltage. In other words,

$$V_s^k = V_{sup}\sqrt{2}\cos\left[\omega t - (k-1)\frac{2\pi}{3}\right] \tag{21}$$

An algorithm to program the above equations can be summarized as follows: For each time step, the values of θ_r and ω_r can be calculated. With θ_r known and voltage for the phases determined, the values of the derivatives of stator and rotor currents can be determined. A Gauss-Jordan back substitution solver can be used to solve the 6x1 current derivative matrix. Next, Eq. (14-19) can be used to determine the derivatives of the mechanical system (θ_m and ω_m). The RK solver can then be invoked to calculate the currents and the mechanical position and angular velocity at each time t. With the currents determined, the motor air-gap torque can be determined. The resulting shaft torques are defined by Eq. (22) and (23).

$$T_{s1} = K_1(\theta_m - \theta_{c1}) \tag{22}$$

$$T_{s2} = K_2(\theta_{c1} - \theta_{c2}) \tag{23}$$

The equations were programmed and solved using Visual Basic with Microsoft Excel as the front end user interface. The per-unit (PU) system for calculations greatly simplifies the calculation procedures. It should be noted that the equations above have been presented for a dual gearbox compressor arrangement to illustrate the procedure for a larger subset; the actual simulations were conducted for a single gearbox drive.

SIMULATION RESULTS

The parameters for the 50 Hz motor connected to a single gearbox compressor mentioned in Appendix I were used for the analytical study. The results of the simulation have been presented in two parts – 3-phase fault and reclosure. In both parts, the motor start from zero to full speed is first simulated and presented in the figures before the appropriate fault is introduced.

When supply voltage is applied across the stator terminals, the motor air-gap torque generated at the rotor terminals oscillates torsionally at line frequency, which in this case is 50 Hz (Fig. 2). The magnitude of this torque can be as high as 4 to 6 times the rated full load torque, depending on the magnitude of the applied voltage. This motor torque gets transmitted to the compressor shaft through the coupling. The shaft torque generated is roughly equal to the ratio of compressor inertia to the total inertia. The length of time it takes for the driven shaft oscillations to die down is a function of the damping in steel, usually 2-4% [8, and based on the author's company's experience] of the critical damping. Figures 3 – 5 show the simulated motor torque, the acceleration time and the shaft torque, for time less than approximately 10.5 seconds.

Although not part of the scope of this paper, it should be noted here that the pulsating torque burst during start for an induction motor is different from that of a synchronous motor. In the latter, the saliency of the poles and the presence of field windings in the motor rotor result in pulsating torques that sweep all frequencies from twice line frequency to zero as the motor starts up. In the case of the induction motor, no such continuous exciting function exists through the start-up process.

Part I: Simulating a 3-phase short and clearing of fault

A 3-phase short circuit is a fault that occurs at the motor terminals. When a 3-phase short circuit occurs, the voltage that is trapped in the motor rotor begins to feed current into the fault for a few (milli) seconds, before it drops down to zero after oscillations. One can imagine this as the response to a step change in input voltage at the terminals from rated value to zero at a certain instant of time for a two degree-of-freedom system. This surge in currents gets translated to the mechanical system via the air-gap torque, resulting in a sudden negative spike in the air-gap torque. The electrical set of equations presented earlier can be modeled for the short circuit case by forcing the voltages in all phases to be zero, when the voltage in phase A passes through a zero going positive [7]. For the simulation results presented in this part, the supply voltage was forced to be zero in all three phases for 20 cycles after the motor had come up to full speed.

The 3-phase fault is simulated in the model once the motor has reached full speed, at approximately 13 seconds from start. Refer Fig. 3-5. The peak motor air-gap torque in this case is approximately -2.5 PU. The disturbance, however, is momentary. The oscillations in currents (and correspondingly the motor and shaft torques) die down fairly quickly. With no voltage supplied to the motor, the motor and the drive train begin to decelerate, as shown in fig. 4. When the fault is cleared (which in this case is simulated after 20 cycles or 0.4 seconds), the voltages are re-applied to the stator terminals. A step change in input voltage from 0 to 1 PU results in the motor torque responding accordingly, with a spike in torque and decay of the oscillations in subsequent cycles. Within this period, the motor returns to its full speed and full load conditions that were present before the occurrence of the fault.

Figure 6 shows the air-gap and shaft torques zoomed in to the time frame during the fault.

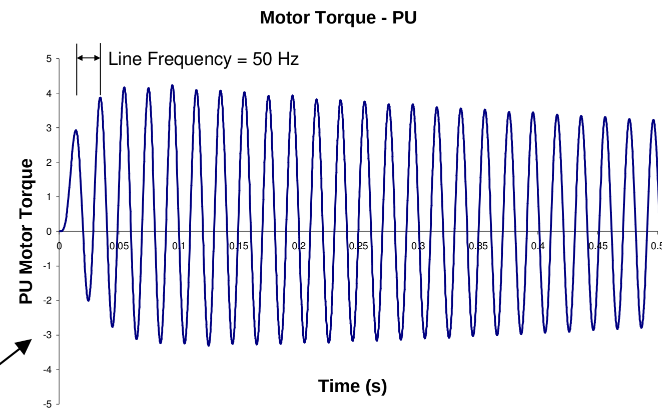

Figure 2: Motor transient torque oscillations at line frequency during start-up

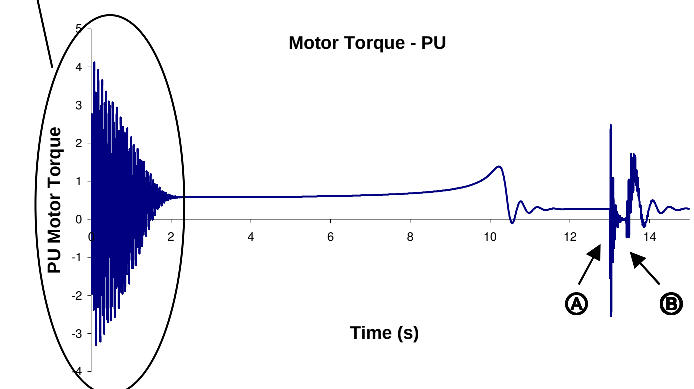

Figure 3: Motor start-up and transient torque

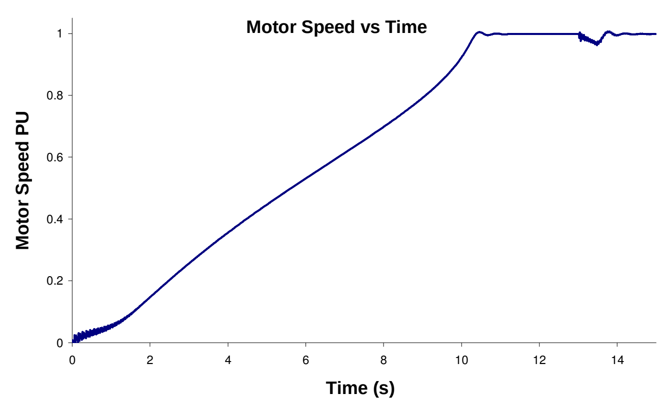

Figure 4: Acceleration time

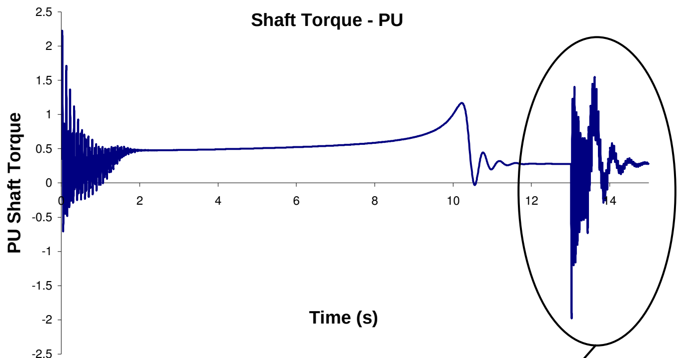

Figure 5: Shaft torque

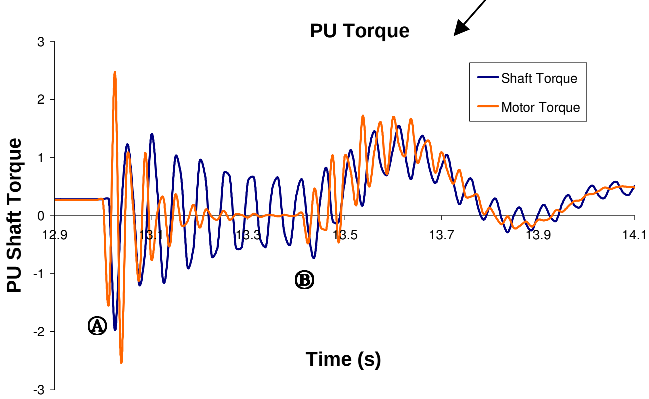

Figure 6: Motor and shaft torques zoomed in during the 3-phase fault; Ⓐ=start of fault, Ⓑ=fault cleared

Part II: Simulating a bus transfer and reclosure

Electrical grids supplying power to industrial sized motors are normally connected to more than a single power transmission supply (known as a bus in power system terminology) to carry power from the master electrical grid to the motors in the system. Faults can occur in the electrical grid or in the lines that carry power from the grid to the sub-station to the motor. When such a fault occurs, it is common to transfer power in the electrical grid from one bus to another. The resultant voltage in the motor rotor during the few seconds when power is lost (from say, grid #1 before its transfer to say, grid #2) begins to decay slowly. The decay rate is governed by the compressor inertia. At the instant power is lost to the system, the currents in the stator drop to zero. This is modeled in the electrical equations described earlier as an "open circuit" by momentarily forcing the stator inductance L_s to a large value, say 10E8 [1]. This forces the derivatives of the currents (and hence the currents) to zero in all three phases.

Although the power input to the motor is cut off due to supply disturbance, the flux trapped in the motor windings does not immediately drop to zero. The rate of decay in the voltage measured at the motor terminals due to this trapped flux is an exponential function of the open circuit time constant $octc$, and is expressed by Eq. (24).

$$V_m = V_{sup} exp^{-t/octc} \qquad (24)$$

where

$$octc = \frac{X_r + X_{mu}}{2\pi f R_r} \qquad (25)$$

This trapped voltage flux not only decays in magnitude, but also progressively begins to lag behind the supply voltage phase angle. This phase lag between the supply voltage and the motor flux voltage at any instant of time is given by Eq. (26).

$$\beta = -\omega_r t \qquad (26)$$

When power supply to the motor is cut off, the motor begins to decelerate at a rate that is governed by the load torque and the total inertia of the system. The value of ω_r at each instant of time for the transient state before reclosure can be calculated from the induction motor equations mentioned before. The resultant voltage due to the trapped flux in the motor at the instant of reclosure is then given by Eq. (27).

$$V_{res} = \sqrt{V_m^2 + V_s^2 - 2V_m V_s \cos\beta} \qquad (27)$$

In the computer simulation presented, a power failure occurs at the grid after the drive train has come up to full speed, at time t = 13 seconds. The bus transfer is simulated to occur after 20 cycles. At the instant the bus transfer occurs, the resultant voltage gets applied to the motor terminals and the motor begins to re-accelerate to full speed. The sudden application of the grid supply voltage (in addition to the voltage due to the trapped flux) results in shaft torsional vibrations that are similar in nature to the one discussed in the previous section. Figures 7 – 9 show the motor torque, acceleration time and shaft torque. Figure 10 shows a detailed view of the motor and shaft torques during reclosure.

DISCUSSION OF RESULTS

The electro-mechanical simulation results reveal the peak shaft torques generated for both the 3-phase and reclosure transients arising from the motor. Representing both the start-up transient and the electrical transient at full speed gives a perspective to compare the peak motor and shaft torques.

In the case of the 3-phase fault simulation (refer fig. 5), the peak torque (~ -2 PU) is of the same magnitude as the start-up transient (~ 2.2 PU) for the case discussed.

In the case of the reclosure simulation, the vector sum of the voltage due to the trapped flux and the supply voltage results in shaft torques that is much higher than the motor torque. The peak shaft torque at reclosure (shown in fig. 9) is of the order of 8 PU, much higher than the transient torque of 2 PU due to the initial burst during start-up. The high reclosure torques reported in this paper is consistent with the findings in the literature [1, 3, 5]. Hizume's [5] analysis was performed for a turbine-generator system. Although the physics of Hizume's

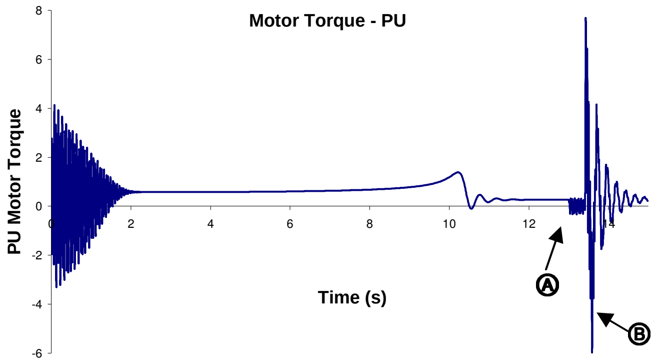

Figure 7: Motor torque

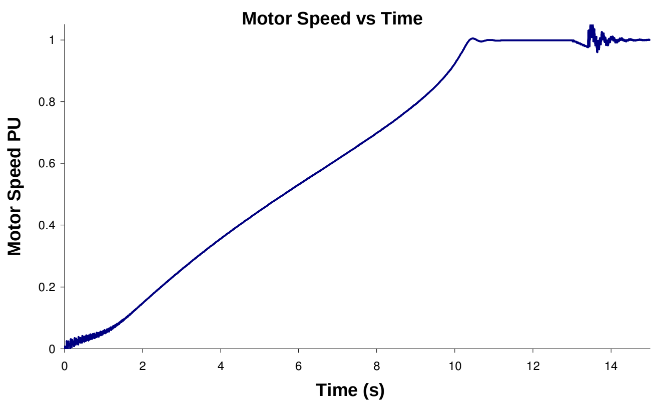

Figure 8: Acceleration time

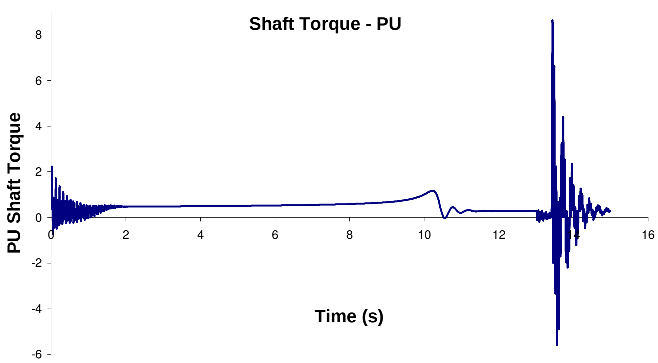

Figure 9: Shaft torque

system and the one presented in this paper are the same, this paper provides a comparison of torques during various faults to the line burst torques during starting. This is especially useful when viewed from the perspective of sizing mechanical components. Also, the analysis in this paper includes damping in the mechanical system, while Hizume's analysis was for zero damping.

The high torques during reclosures place severe constraints on the coupling and sometimes end up shearing the coupling, coupling keys or drive shafts. In the author's company's experience, damage has been noted to the gear teeth in the compressor due to reclosure transients in certain extreme cases.

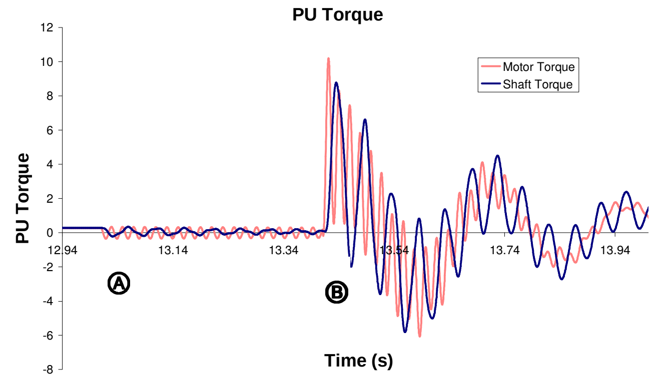

Figure 10: Motor and shaft torque during reclosure, zoomed in

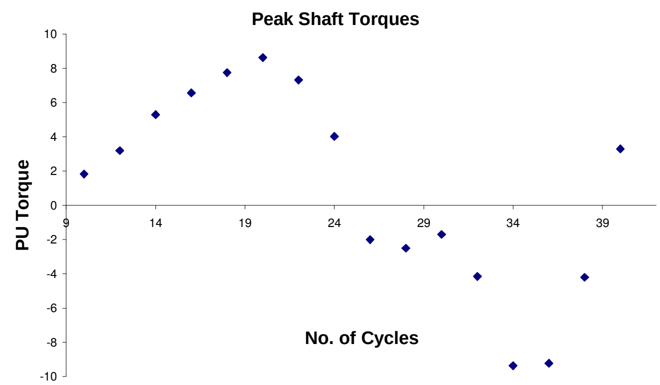

Figure 11: Peak shaft torque for various cycles before reclosure

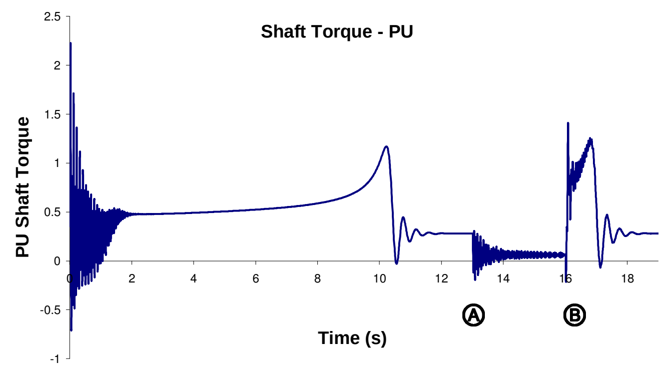

Figure 12: Motor torque for 150 cycles before reclosure

In order to understand the effect of the number of cycles on shaft torques, the study was repeated for a range of cycles, and the shaft torques were plotted. Figure 11 shows one such plot of the peak shaft torque versus number of cycles before reclosure occurs. Of particular interest is the fact that the predicted shaft torque is less than the peak torque at start-up for certain ranges of number of cycles (9 to 12 and 26 to 30 in this case).

However, at other instances (at number of cycles near 20 and 36 before reclosure), the peak shaft torque is much higher than that during start-up. This result also makes sense upon re-examining Eq. (27); the time dependant nature of V_{res} results in an exponential-cosine decay, with V_m and V_s being additive vectors (i.e., in-phase) at certain instances and out of phase at other instances of time.

As the time between bus transfers increases, (i.e., as the number of cycles before reclosure increases), the trapped flux in the air-gap dissipates to a low enough level. This reduced voltage from the air-gap of the motor reduces the effect of the peak transient generated due to reclosure. Figure 12 combines the shaft torque start-up response and the response for 150 cycles (or 3 seconds) before reclosure. The peak shaft torque at reclosure is approximately 1.5 PU, which is much lower than that for the 20-cycle reclosure case. For a mechanical system, this result makes practical sense since the inertial effect on shaft torque at full speed is much greater than that at a slower speed. Thus, the system response to an impulse function will be a lower value at slower speeds.

CONCLUSIONS

The 3-phase model of an induction motor has been adapted to simulate and investigate the effects of start-up and transient upsets during steady state running condition, and its effect on compressor drive train shaft torques. The electrical equations for angular velocity and angular displacement have been related to the mechanical counter parts by the pole pairs. The mechanical system of equations has been modeled using the fundamental laws of motion.

It has been shown analytically that in certain cases, the peak shaft torques created by upsets in the electrical system can place severe constraints for OEM equipment such as compressors. Although it is understandable from a process industry point of view to keep machinery running continuously without complete shut downs during power interruptions, careful simulations such as the one presented in this paper may need to be evaluated on a case-by-case basis to understand the magnitudes of the peak torques generated.

Adequate caution must be exercised in the use of such modeling procedures. A cursory glance at Fig. 11 may possibly mislead the reader to assume that reclosures are theoretically possible for certain instances of number of cycles when the predicted shaft torque magnitude is comparable to the coupling rating. However, extraneous factors such as non-linearities in the induction motor have not been taken into account and are well beyond the scope of this paper. Methods that exist in the electrical engineering literature that control the exact instant of time when the bus transfer can be made to occur require a more detailed electro-mechanical analysis, and are also beyond the scope of this paper.

While the coupling for the machinery drive train can be sized to withstand known transient conditions such as those during start-up, sizing couplings and drive-train shafts for other electrical transients such as the ones discussed above may not always guarantee risk-free operation. In several cases, it may not even be practical to size machinery components for such upsets. Going with a conservative approach of shutting down the drive train in the event of an electrical disturbance, rather than attempting to clear the fault on-the-fly, could save both money and potential lost time due to down machines.

REFERENCES

[1] Daugherty R. H., 1982, "Analysis of transient electrical torques and shaft torques in induction motors as a result of power supply disturbances" IEEE Trans. On Power App. Sys., Vol PAS-101, No. 8, pp 2826-2836.

[2] Daugherty R. H., 1990, "Bus transfer of AC induction motors: a perspective", IEEE Trans. on Ind. App., Vol. 26, No. 5, pp. 935-943.

[3] Mruk G., Halloran J., 1988, "Torques due to electrical reclosures for induction motor driven centrifugal compressors", Proc. Vibration Institute 12th Annual Meeting, May 25-27, pp 185-189.

[4] Shaltout A., Al-Omoush M., 1996, "Reclosing torques of large induction motors with trapped flux", IEEE Trans. on Energy Conversion, Vol 11, No. 1, pp 84-90.

[5] Hizume A., 1975, "Transient torsional vibration of steam turbine and generator shafts due to high speed reclosing of electric power lines", ASME 75-DET-71, pp 968-979.

[6] Melfi M., Umans S., 2010, "Transients during line-starting of squirrel cage induction motors", IEEE IAS PCIC 57th annual conference, paper no. PCIC-2010-23.

[7] Krause P., Wasynczuk O. and Sudhoff S., 1994, "Analysis of electric machinery", IEEE Press.

[8] Vance J., 1988, "Rotordynamics of Turbomachinery", Wiley Publication, Chapter 3.

[9] Fitzgerald A. E., Kinglsey Jr. C., Umans S., 1990, "Electric Machinery", McGraw Hill, 5th ed.

APPENDIX

The data for the motor used were as follows:
6000 V, 4160 HP, 2 pole, 50 Hz induction motor.
The electrical parameters used were:

PU parameters	Locked rotor	Full speed
R_s	0.006	0.063
R_r	0.024	0.005
X_s	0.135	0.135
X_r	0.063	0.105
X_{mu}	5.752	4.641

Mechanical parameters: $J_m = 26$ lb-ft-s^2, $J_{c1} = 87$ lb-ft-s^2, $K_1 = 303{,}500$ lb-ft/rad, $C_1 = 2\%$ of critical damping, $FLT_{c1} =$ 6900 ft-lb.

The electrical quantities are non-dimensionalized by dividing the appropriate quantity by its base quantity.

The PU supply voltage of 1.0 corresponds to 6000 V.

The PU torque is obtained by dividing the appropriate torque by the base motor torque, i.e.,

$$T_{base} = \frac{5252*4160}{rpm} \text{ ft-lb, where}$$

$$rpm = \frac{120\, f}{Poles}$$

The PU base speed is 1 rad/s. A more detailed explanation of the PU system can be found in [7].

ACKNOWLEDGMENTS

The author would like to thank Cameron Process and Compression Systems for their permission to publish this paper.